Transporter-to-Trap Conversion: a Disulfide Bond Formation in Cellular Retinoic Acid Binding Protein I Mutant Triggered by Retinoic Acid Binding Irreversibly Locks the Ligand Inside the Protein†

Virginie Sjoelund and Igor A. Kaltashov*

Department of Chemistry and Molecular and Cellular Biology Program, University of Massachusetts at Amherst, Amherst, Massachusetts 01003

Received May 7, 2007; Revised Manuscript Received September 5, 2007

ABSTRACT: Transport proteins must bind their ligands reversibly to enable release at the point of delivery, while irreversible binding is usually associated with the extreme cases of ligand sequestration. Protein conformational dynamics is an important modulator of binding kinetics, as increased flexibility in the regions adjacent to the binding site may facilitate both association and dissociation processes. Ligand entry to, and exit from, the internal binding site of the cellular retinoic acid binding protein I (CRABP I) occurs via a flexible portal region, which functions as a dynamic aperture. We designed and expressed a CRABP I mutant (A35C/T57C), in which a small-scale conformational switch caused by the ligand binding event triggers formation of a disulfide bond in the portal region, thereby arresting structural fluctuations and effectively locking the ligand inside the binding cavity. At the same time, no formation of the disulfide bond is observed in the apo form of the mutant, and most characteristics of the mutant, including protein stability, are very similar to those of the wild-type protein in the absence of retinoic acid. The mutation does not alter the kinetics of retinoic acid binding to the protein, although the disulfide formation makes the binding effectively irreversible, as suggested by the absence of retinoic acid transfer from the holo form of the mutant to lipid vesicles in the absence of a reducing agent. Taken together, these data suggest that the disulfide bond formation in the portal region arrests large-scale structural fluctuations, which are required for retinoic acid release from the protein. The unique properties of the CRABP I mutant described in this work can be used to inspire and guide a design of nanodevices for multiple tasks ranging from sequestering small-molecule toxins in both tissue and circulation to nutrient deprivation of pathogens.

Retinoic acid (RA),[1] a metabolite of vitamin A, exerts a wide variety of effects on vertebrate development, cellular differentiation, and homeostasis (*1*−*4*). Clinically it is used for treatment of skin disorders, prevention of epidermal cancer, and treatment of acute promyelocytic leukemia (APL) (*5*, *6*). RA modulates gene expression via binding to nuclear receptors, which belong to the steroid/thyroid hormone superfamily and act as transcription factors (*1*, *7*−*9*). In addition, there are two low molecular weight intracellular proteins interacting with RA. These are the cellular retinoic acid binding proteins (CRABP I and CRABP II), which belong to the family of intracellular lipid-binding proteins (iLBPs). The functions attributed to CRABPs are to solubilize RA in the cytosolic environment and either transport it to the nuclear receptor site or modulate the amount of free RA available to the nuclear receptors by sequestering it in the cytosol (*10*, *11*).

All members of the iLBP family are characterized by a conserved structure, which is formed by two orthogonal β-sheets (each composed of five antiparallel β-strands) with a helix−turn−helix motif inserted between them. The β-barrel contains a poorly accessible hydrophobic ligand-binding cavity. Entry of RA into the cavity of CRABPI is believed to occur via a region of the protein comprising the βC−D loop, the βE−F loop, and the N-terminal region of helix II (*12*). It is usually referred to as the portal region of CRABP and has been extensively studied in other members of the iLBP family, in particular in the fatty acid binding protein, by X-ray crystallography, mutational analysis, and multidimensional NMR (*13*−*16*). NMR and mass spectrometric studies have shown that the backbone flexibility in the portal region of CRABP I is very significant (compared to the rest of the polypeptide chain) in the apo form of the protein and decreases dramatically upon RA binding (*12*, *17*). These observations support the notion that the portal region is dynamic in nature and undergoes rapid fluctuations, where transient loss of structure allows RA to enter the cavity housing the internal binding site, which is inaccessible in the static structure of the protein.

† This work was supported by a grant from the National Institutes of Health (R01 GM061666).

* Address correspondence to this author: Department of Chemistry, University of Massachusetts, 710 North Pleasant St., Lederle Graduate Research Tower #701, Amherst, MA 01003. Tel: (413) 545-1460. E-mail: kaltashov@chem.umass.edu.

[1] Abbreviations: CRABP, cellular retinoic acid binding protein; RAR, retinoic acid receptor; RA, retinoic acid; IFABP, intestinal fatty acid binding protein; iLBP, intracellular lipid binding protein; MS, mass spectrometry; ESI, electrospray ionization; DOPC, 1,2-dioleoyl-*sn*-glycero-3-phosphocholine; CD, circular dichroism; IPTG, isopropyl β-D-1-thiogalactopyranoside; LB, Luria broth; CAD, collision activation dissociation; BME, β-mercaptoethanol; SUV, small unilamellar vesicles; TCEP, tris(2-carboxyethyl) phosphine.

10.1021/bi700867c CCC: $37.00
Published on Web 10/24/2007

Recent studies of the intestinal fatty acid binding protein (another member of the iLBP family) led to a suggestion that, once the hydrophobic ligand has entered the binding cavity, it is kept within its confines via multiple contacts to residues on the α-helix II and the βC−D loop. Furthermore, comparison of the crystal structures of apo- and holo-CRABP I showed that, upon binding, the βC−D loop moves closer to the α-helix II (*18*−*20*). However, the association process is reversible, as the noncovalent protein−ligand interactions only decrease, but do not completely eliminate, the transient unfolding events in the portal region, which now provide a route to complex dissociation. The main objective of this work was to engineer a mutant whose conformational properties (both structure and dynamics) are indistinguishable from those of the wild-type protein in the absence of the ligand, while the mobility in the portal region is eliminated in the holo form. Since both passive and active RA transfers from CRABPs to RAR (*21*) are important elements in transcription modulation, availability of a CRABP mutant that freely binds the ligand, but fails to release it under physiological conditions, would be a valuable instrument in our ongoing studies of the receptor−transporter interactions.

We hypothesized that if we could physically arrest fluctuations in the portal region and effectively lock the protein in the holo conformation, RA would not be able to escape from the internal cavity. We found two residues, located in the α-helix II and in the βC−D loop, that upon mutation to cysteines could form a disulfide bond only in the holo form, thus creating a covalent cross-link, which cements the holo conformation of the protein, thereby preventing RA exit from the binding cavity. While the oxidation of the two strategically placed cysteine residue occurs readily in the holo form of CRABP I mutant, no disulfide bond forms in the absence of the ligand, as the geometry of the apo conformation of the protein does not allow the two thiol groups to interact. The selective ability of this mutant to form a conformation-constraining cross-link only after the ligand binding event allows RA to be locked inside the protein cavity without obstructing its entry to the binding site. In addition to providing further support for the portal model of CRABP−RA interaction, the results of this work can be used to inspire design of therapeutic agents with precisely tuned properties for multiple tasks in nanomedicine ranging from sequestering small-molecule toxins in both tissue and circulation to nutrient deprivation of pathogens.

MATERIALS AND METHODS

Bacterial Strains and Plasmids. A previously constructed plasmid, pET-CRABP I (*18*), containing the CRABP I gene subcloned in the *Escherichia coli* expression vector pET-16b (Novagen, San Diego, CA) was used for site-directed mutagenesis and overexpression of both wild-type and mutant CRABP I. The pET-16b vector contains an N-terminal His tag and a short linker with a factor Xa cleavage site. *E. coli* DH5α was used as the host strain for propagating the recombinant plasmids carrying the CRABP I wild-type and mutant gene. *E. coli* BL21 (DE3), having a copy of the T7 RNA polymerase gene on its chromosome, was used as the host strain for overexpression of both wild-type and mutant CRABP I.

Site-Directed Mutagenesis. The A35C/T57C mutant was constructed by site-directed mutagenesis via the inverse-PCR method (*22*). The oligonucleotides (Integrated DNA Technologies, Coralville, IA), templates, and mutant constructed are shown in Supporting Information. The PCR reactions (50 μL) consisted of 50 ng of the DNA template, 0.25 μM forward primer, 0.25 μM reverse primer, 25 μM of each deoxynucleoside triphosphate (Gibco BRL, Carlsbad, CA), 1× *Pfu*I buffer (Stratagene, La Jolla, CA), and 2.5 units of *Pfu*I polymerase (Stratagene) and were subjected to the following program; denaturation (95 °C for 1 min), amplification 16× (95 °C for 30 s, 55 °C for 1 min, 68 °C for 13 min), and extension (68 °C for 30 min). At the end of the PCR cycle, 45 μL of the product was digested with *Dpn*I at 37 °C for 1 h. Both the digested and nondigested DNA were separated on a 1% agarose gel; a band corresponding to the full-length plasmid (6.4 kb) was present as the only significant product. The DNA was used to transform the *E. coli* strain DH5α, which was plated onto LB agar containing 0.1 mg/mL ampicilin. The plasmid from the transformants was extracted by use of the QIAprep spin miniprep kit (Qiagen, Valencia, CA) and checked by DNA sequencing whether the plasmids have incorporated the right mutation and have maintained fidelity throughout the rest of the gene sequence.

Protein Expression. Wild-type CRABP I and CRABP I-A35C/T57C were expressed in *E. coli* BL21 (DE3) cells. Expression cultures (1 L of LB medium supplemented with 1 μg/mL ampicillin), inoculated from a culture grown to an OD_{600} of 1.0 at a 1:25 dilution, were grown at 37 °C, 250 rpm, until the OD_{600} reached ≈0.7. Protein expression was induced with 0.4 mM IPTG for 3 h at 37 °C for wild-type CRABPI and 30 °C for the A35C/T57C mutant. The protein purification process has been described elsewhere (*18*).

Circular Dichroism. The CD spectra were measured with a Jasco J-715 spectropolarimeter (Jasco, Tokyo, Japan). Solutions with a protein concentration of 10 μM in 10 mM sodium phosphate buffer (pH 8.0) were placed in a 1 mm quartz cuvette for far-UV experiments (195−250 nm). Each spectrum was obtained by scanning this range with 0.5 nm increments at a 20 nm/min rate; five runs were averaged for each spectrum to ensure adequate signal-to-noise ratio. After buffer baseline subtraction, the CD data were normalized to protein concentration and expressed as molar residue ellipticity.

Membranes. 1,2-Dioleoyl-*sn*-glycero-3-phosphocholine (DOPC) was obtained from Avanti Polar Lipids (Alabaster, AL). Small unilamellar vesicles of DOPC were prepared by sonication. DOPC in chloroform was pipetted into a glass tube and the solvent was evaporated under a stream of nitrogen. The lipid film was further dried under vacuum for 30 min. The lipids were resuspended in buffer containing 10 mM Tris and 100 mM NaCl (pH 8.0), and the suspension was sonicated until it was clear.

Fluorescence Titrations. The binding properties of the mutant protein were measured by a fluorometric titration method (*23*) (FelixX32, PTI, Lawrenceville, NJ). Wild-type and mutant proteins (1 μM in 10 mM Tris buffer, pH 8.0) were excited at 280 nm and the emission spectra were recorded in the 300−380 nm range (2 nm slit width). Concentrated RA solution in ethanol was added to the protein solutions in 3 μL aliquots. The final volume of added ethanol

did not exceed 1.7% of the protein solution total volume. Concentration of RA stock was determined spectrophotometrically using a molar absorption coefficient of 45 000 M^{-1} cm^{-1} at 336 nm (*23*).

Rate of Association of Retinoic Acid with CRABPI A35C/T57C. Solutions of apo-CRABP I and apo-CRABP I mutant A35C/T57C (1 μM each in a buffer containing 10 mM Tris, pH 8.0) were placed in fluorescence cuvettes. Retinoic acid from a 1 mM stock was added to each cuvette to a final concentration of 1 μM, and the fluorescence intensity at 328 nm (excitation at 280 nm) was followed at 1.45 s time intervals until the equilibrium was reached.

Binding of RA to the protein is a second-order reaction, whose rate can be expressed as k_{on}[protein][RA]. If the initial concentrations of the two binding partners are equal to each other ([protein]$_0$ = [RA]$_0$ = 1 μM), then

$$\frac{1}{RA} - \frac{1}{RA_0} = k_{on}t \tag{1}$$

Concentration of free [RA] in solution can be calculated at any point in time from the fractional concentrations of the apo and holo forms of the protein:

$$\alpha = \frac{F_{apo} - F}{F_{apo} - F_{holo}} \tag{2}$$

where F_{holo} and F_{apo} are fluorescence intensities of the end points of the ligand binding reactions (the apo- and holo-proteins). F is the fluorescence of the protein at a given retinoic acid concentration. The fluorescence data sets were fitted to eqs 1 and 2 to obtain the k_{on} value of the association reaction.

Rate of Transfer of Retinoic Acid between CRABPI A35C/T57C and Vesicles. A reduced mixture of CRABP I mutant A35C/T57C with retinoic acid (1:1 molar ratio) was mixed in a cuvette with 3.2 mM DOPC vesicles in a buffer containing 10 mM Tris, 100 mM NaCl, and 1 mM BME, pH 8.0. The final volume of the mixture was 1 mL. Fluorescence intensity at 328 nm (excitation at 280 nm) was followed at 5 s time intervals until equilibrium was reached. Since the dissociation reaction follows first-order kinetics with a rate constant k_{off}, the latter could be obtained by fitting the fluorescence data set to the following equation:

$$\ln (F_{apo} - F) = - k_{off}t \tag{3}$$

Distribution of Retinoic Acid between CRABP I A35C/T57C and DOPC Vesicles. Mixtures of reduced and nonreduced CRABP I A35C/T57C with retinoic acid (1:1 molar ratio) were mixed in cuvettes with DOPC vesicles (the DOPC concentration in solution was 3.2 mM) in a buffer containing 10 mM Tris, 100 mM NaCl, and 1 mM BME to a final volume of 100 μL. The intensity of the fluorescence signal was monitored at 328 nm for 5 min at equilibrium every 5 s (excitation at 280 nm). The amount of RA present in the vesicles versus that bound to the protein was obtained by calculating the theoretical fluorescence for the apo and holo forms in the presence of small unilamellar vesicles (SUV):

$$F_{apo}{}^{SUV} = F^{SUV} + F_{apo} - F_{buffer} \tag{4a}$$

$$F_{holo}{}^{SUV} = F^{SUV} + F_{holo} - F_{buffer} \tag{4b}$$

where F^{SUV}, F_{apo}, and F_{holo} are the fluorescence of the SUV alone, the apo form in the absence of SUV, and the holo form in the absence of SUV, respectively.

The fraction of RA transferred from the protein to the vesicles can be calculated as

$$\alpha = \frac{F_{apo}{}^{SUV} - F^{SUV}}{F_{apo}{}^{SUV} - F_{holo}{}^{SUV}} \tag{5}$$

Peptide Mapping and Disulfide Detection/Localization. Apo and holo forms of mutant CRABP were treated with excess iodoacetic acid (Acros Organics, Morris Plains, NJ) for 90 min, in the dark, at room temperature to protect any free cysteines. The reaction was ended by removal of the excess iodoacetic acid by running the protein through a desalting column. Immobilized TPCK [L-(tosylamido-2-phenyl)ethylchloromethyl]trypsin was obtained from Pierce Biotechnology Inc. (Rockford, IL) and washed 3 times with 100 mM NH_4HCO_3/NH_4OH solution at pH 8.0 prior to digestion. Protein digestion was initiated by dispersing the immobilized trypsin in 50 μM apo- or holo-CRABP I A35C/T57C solutions in 100 mM NH_4HCO_3 (pH 8.0). Digestion was carried out for 3 h at 37 °C in the dark (to protect RA from possible photoisomerization). Proteolysis was stopped by removing the immobilized TPCK from the protein solution by centrifugation and subsequent freezing of the supernatant.

Masses of tryptic fragments of CRABP I A35C/T57C were obtained with a Qstar-XL (ABI-Sciex, Foster City, CA) hybrid quadrupole/time-of-flight mass spectrometer in the positive ion mode. Tryptic peptide solutions were continuously infused into the TurboSpray source at a flow rate of 5 μL/min. Presence of a disulfide bond-linked peptide dimer among the proteolytic fragments was detected by collision-activated dissociation (CAD) in the negative ion mode following mass selection of a precursor ion. Stability of protein−RA complexes in the gas phase was evaluated by monitoring the extent of complex dissociation as a function of declustering potential (DP) in the ESI interface (10−60 V).

RESULTS

Rationale of Mutant Design. The crystal structures of apo- and holo-CRABP I show that ligand binding does not result in a large conformational change. However, the portal model of RA binding suggests that the protein−ligand association event triggers relatively small-scale repositioning of several segments including helices αI and αII and turns between βC−D and βE−F (*18*, *22*). We used the crystal structures of the holo and apo forms of CRABP I to search for residues within and/or near the portal region that are distant from each other in the apo form (1CBI), but are brought in close proximity as a result of the conformational readjustment following RA binding (1CBR). The proximity should be close enough to afford formation of a disulfide bond, should each of these two residues be mutated to a cysteine. The amino acid sequence of the wild-type CRABP I was screened to identify such a residue pair(s) by use of the geometry-

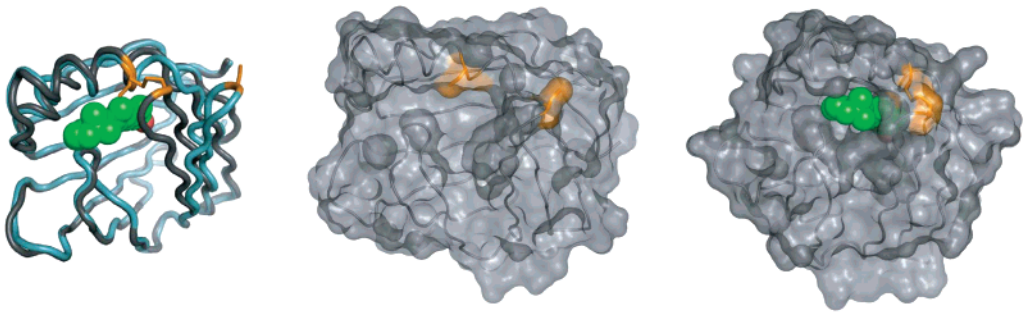

FIGURE 1: Hypothetical structures of CRABP I A35C/T57C built on the CRABP I backbone (1CBI for the apo form and 1CBR for the holo form). (Left) Superimposed backbone traces of the apo (cyan) and holo (gray) conformations of the protein. (Center) Surface model of apo-CRABP I A35C/T57C with the introduced cysteine residues shown in orange. (Right) Model of holo-CRABP I A35C/T57C with the cysteine residues shown in orange and RA shown in green.

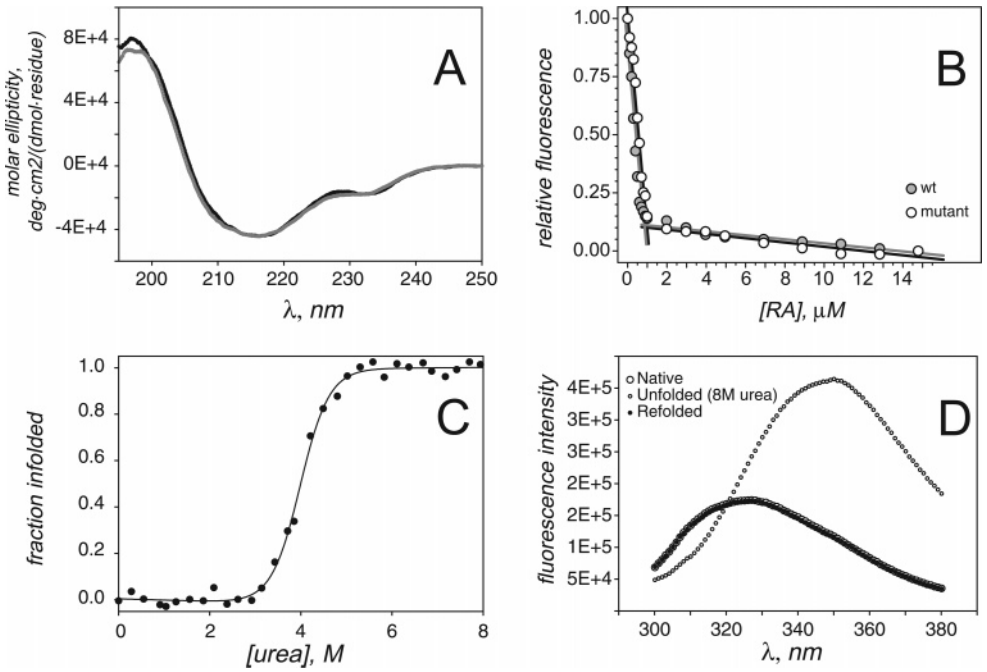

FIGURE 2: (A) Far-UV CD spectra of CRABP I (black trace) and CRABP I A35C/T57C (gray trace). For each spectrum, the protein concentration was 10 μM and the buffer was 10 mM sodium phosphate, pH 8.0. The spectra were collected for the apo forms of the proteins at 25 °C and were baseline-corrected by subtracting a blank spectrum. (B) Fluorometric titration of CRABP I and CRABP I A35C/T57C with RA. The normalized fluorescence for each protein (1 μM) at 328 nm in 10 mM Tris, pH 8.0, at room temperature in the presence of increasing amounts of RA is shown. (C) Urea-induced unfolding of CRABP I A35C/T57C. Denaturation was monitored as the change in the fluorescence emission intensity at increasing concentrations of urea (10 μM protein, λ_{ex} = 280 nm). Raw fluorescence was converted to the fraction of unfolded protein. (D) Fluorescence emission spectra of the mutant protein in the native form (○), denatured in 8 M urea (◦), and after refolding from 8 M urea back to native conditions (•).

based disulfide by design program (*51*). Among all possible combinations, only pairs located on two different segments of the protein, one located in the portal region, were considered. Pairs capable of forming a disulfide bond in both the apo and holo forms were also eliminated. That left only one pair (A35 on helix αII and T57 on the turn βC−D) (Figure 1). These two residues are in close enough proximity in the holo form to make a disulfide bond but not in the apo form. It is noteworthy that neither A35 nor T57 is involved in interactions with the ligand.

Expression and Purification of the Mutant Protein. The CRABPI A35C/T57C mutant was constructed in a CRABP I wild-type (wt) background that contained an N-terminal His tag to facilitate its purification (see Supporting Information). As was the case for the wt-CRABP I, the mutant overexpressed well in *E. coli* and partitioned to the cytoplasm, rendering the purification a one-step process on a Ni-NTA column. Typical yields for wt-CRABP I and the mutant protein were 30 mg/L of cell culture and 20 mg/L cell culture, respectively.

CD Spectra Correspond to β-Sheet Proteins. Far-UV CD spectra for both wt and mutant CRABP I show a minimum at 216 nm and a maximum at about 197 nm (Figure 2A), which is characteristic of β-sheet proteins. In addition, the CD spectra for WT shows a trough at 228 nm, which has been shown to arise from fine details in the tertiary structure surrounding W87 and W109 (*24*). These characteristics are also present in our mutant protein. When the protein is complexed with RA in the presence or absence of a reducing agent (see Supporting Information), there is no significant change in the CD spectra, indicating that the mutation, whether the protein is in an apo or holo form, does not induce significant changes in its secondary structure.

Stoichiometry of RA Binding to CRABP I Is Not Affected by the Mutation. In order to ascertain that the mutant retained the ability to bind RA, fluorescence titrations were carried

Table 1: Kinetic and Thermodynamic Parameters of wt-CRABP I and the Double Mutant A35C/T57C

	wt-CRABP I	A35C/T57C	
		no reducing agent in apo or holo forms	BME present in both forms
ΔG, kcal/mol	7.33 ± 0.45	7.29 ± 0.55	not measured
m, kcal/(mol·M)	1.93 ± 0.11	1.89 ± 0.13	not measured
C_m, M	3.80 ± 0.02	3.86 ± 0.03	not measured
k_{on}, 10^6 (M·min)$^{-1}$	61.1 ± 0.8	60.2 ± 1.1	61.4 ± 0.7
k_{off}, min^{-1}	0.22 ± 0.01[a]	not measured	0.31 ± 0.1
K_d, nM	3.6 ± 0.12	not calculated	5.05 ± 0.10

[a] Taken from ref *10*.

out for both wt-CRABP I and the A35C/T57C mutant. The intrinsic fluorescence of various retinoid-binding proteins, including CRABP I, decreases upon ligand binding due to the overlap from the fluorescence emission bands of tryptophan and tyrosine side chains and the absorption bands of retinoids. Consequently, if a tryptophan side chain is positioned in the vicinity of the ligand binding site, fluorescence quenching ensues upon ligand binding. This phenomenon has been extensively studied and used to monitor binding of retinoids to a variety of proteins, including CRABP I (*23*−*27*). The mutant CRABP I binds retinoic acid with the same stoichiometry as wt-CRABP I (Figure 2B). Both the wild-type and the mutant protein are 50% in the holo form at a concentration of RA that is 50% of that of the protein, showing that no RA is free, and thus the binding stoichiometry is 1:1. Since the protein concentration used is significantly above published K_d values, these data cannot be used to measure the K_d of the reaction.

Unfolding of the Mutant Is Cooperative and Reversible in the Absence of RA. To examine whether the double mutation altered the global conformational stability of CRABP I, the sensitivity of the mutant to urea-induced denaturation was determined. Urea-induced unfolding of CRABP I is associated with a red shift in the emission spectra of the protein and an increase in the fluorescence intensity (Figure 2D). Previous work has shown that the presence of the His tag does not perturb the structure (*18*). The mutant unfolded cooperatively and refolded reversibly (Figure 2C). The equilibrium data are well described by a two-state folding process (*28*). The urea sensitivity of the mutant is essentially the same as that of wt-CRABP I, strongly suggesting that the double mutation did not affect the overall conformational stability of the protein (Table 1).

Formation of a de Novo Disulfide Bond in the Holo Form of the Double Mutant. In order to verify disulfide bond formation between the two introduced cysteine residues following RA binding to the double mutant, disulfide mapping was carried out both in the presence and in the absence of retinoic acid in the protein solution. The protein was treated with iodoacetic acid, followed by trypsin digestion and ESI-MS analysis of the masses of the proteolytic fragments. The tryptic digest of the double mutant in the absence of RA contained 19 peptides, 16 of which were at least three amino acid residues long and were easily assigned (see Supporting Information for more detail). Two of these peptides (T7 and T9) were notably absent in the digest of the protein treated with iodoacetic acid in the presence of RA. Instead, an additional species was present, whose mass corresponded to a peptide dimer T7/T9 linked by a disulfide bond (Figure 3).

The identity of this species and the presence of a disulfide bond were verified by fragmenting it in the negative ion mode. Unlike collision-induced dissociation (CAD) of peptide cations, fragmentation in the negative ion mode usually leads to facile dissociation of disulfide bonds, resulting in highly recognizable "signature" dissociation patterns of peptide oligomers containing external disulfide cross-links (*20*, *29*). Figure 4 shows the CAD spectrum of a dianionic species at m/z 1071, where the three major groups of fragment ions represent anionic species corresponding to T7 and T9 segments of the protein, unequivocally confirming identification of this tryptic peptide as a disulfide-linked T7/T9.

The Double Mutant Traps Retinoic Acid inside the Binding Cavity under Nonreducing Conditions: Rate of Association of Retinoic Acid with CRABP I A35C/T57C. The rate constant of association of retinoic acid with CRABPI A35C/T57C (k_{on}) was measured by utilizing the quenching effect of retinoic acid on the protein upon binding (*23*). Retinoic acid was dissolved in ethanol and mixed with wt-CRABP I and the mutant. The fluorescence of each mixture at 328 nm (excitation at 280 nm) was monitored at 1.45 s intervals until the equilibrium was reached. Since the initial concentrations of both the protein and retinoic acid in these experiments were the same, and the binding stoichiometry is 1:1 for both wild-type protein and the mutant (vide supra), the second-order rate constants of protein−ligand association can be obtained by plotting $1/[RA]_t - 1/[RA]_0$ as a function of time (Figure 5A). No significant difference in the binding kinetics was observed between wt-CRABP I and the double mutant, suggesting that the mutations had no effect on the binding kinetics of retinoic acid into the cavity of the protein (Figure 5B). Furthermore, addition of the reducing agent to the mixture of RA and the double mutant had no effect on the binding kinetics. The k_{on} values obtained in this experiment are as follows: $(61.1 \pm 0.8) \times 10^6$ (M·min)$^{-1}$ and $(61.4 \pm 0.7) \times 10^6$ (M·min)$^{-1}$, respectively, for the wild-type and mutant proteins in the absence of the reducing agent and $(61.2 \pm 1.1) \times 10^6$ (M·min)$^{-1}$ and $(60.2 \pm 1.1) \times 10^6$ (M·min)$^{-1}$ for the wild-type and mutant proteins in the presence of 0.1 mM TCEP. These results clearly indicate that the side chains of the introduced cysteine residues do not interfere with the ligand entry into the cavity in the apo form of the double mutant.

RA Partitioning between Membranes and Protein in Reducing and Nonreducing Environments. Poor solubility of RA in water makes it difficult to monitor its dissociation from CRABP I in aqueous environments. In order to avoid this problem, RA dissociation from the double mutant of CRABP I was monitored in the presence of a "hydrophobic

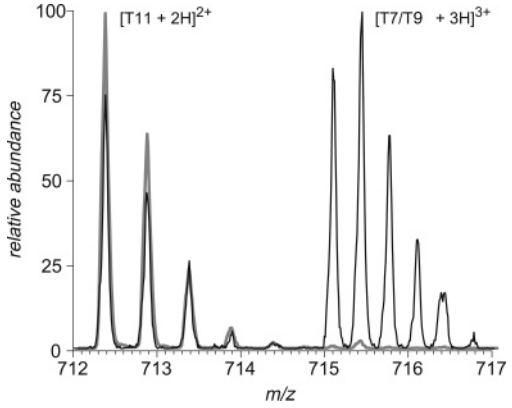

FIGURE 3: Positive ion ESI MS of tryptic digests of apo- (gray trace) and holo- (black trace) CRABP I A35C/T57C, showing *m*/*z* region corresponding to the T11 and T7/T9 peptide fragments.

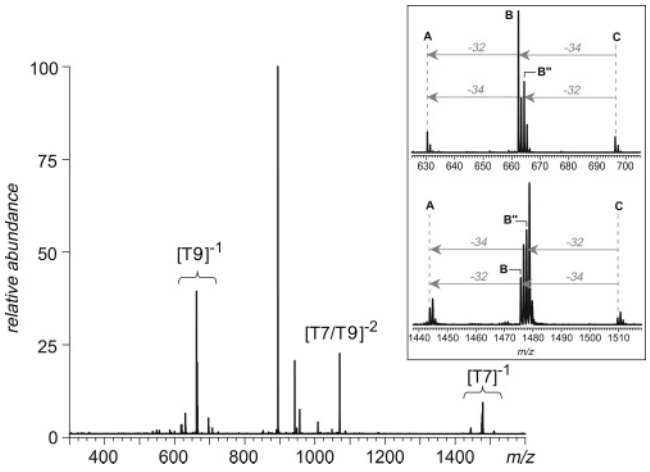

FIGURE 4: Negative CAD MS of a doubly charged peptide dimer $[T7/T9 - 2H]^{2-}$ showing a characteristic dissociation pattern arising due to the gas-phase cleavage of the disulfide bond connecting peptides T7 and T9.

sink", chosen to be unilamellar DOPC vesicles. This system has been previously used to monitor the dissociation of the CRABP/RA complexes (*10*) and of retinoid binding proteins/retinoids in general (*26*, *30*, *31*). Since the presence of vesicles had no effect on the intrinsic fluorescence of the protein (see Supporting Information for more detail), RA transfer from the protein to the vesicles could be followed by monitoring the increase in fluorescence of the protein. These experiments do not aim at measuring the k_{off} value but at ascertaining whether RA partitions from the protein to the vesicles. The fluorescence change is shown in Figure 6 (top). In the presence of 1 mM BME, the fluorescence after 10 min is indistinguishable from that of the protein in its apo form. Without a reducing agent, the fluorescence after 10 min remains at level of the holo form. The amount of apoprotein in the presence of the reducing agent is (96.3 ± 1.1)% and in the absence of reductant is (4.1 ± 0.6)% (Figure 6, bottom). The disulfide bond present in the holo form efficiently "traps" retinoic acid in the binding cavity on the time scale of these experiments.

Since RA does not dissociate from the double mutant in the absence of the reducing agent, measurement of k_{off} had to be done under reducing conditions (Figure 7). The measured off rate is 0.311 ± 0.004 min^{-1}, which is in good agreement which previous published results for the wild-type protein (*32*). The resulting apparent K_d for the reduced

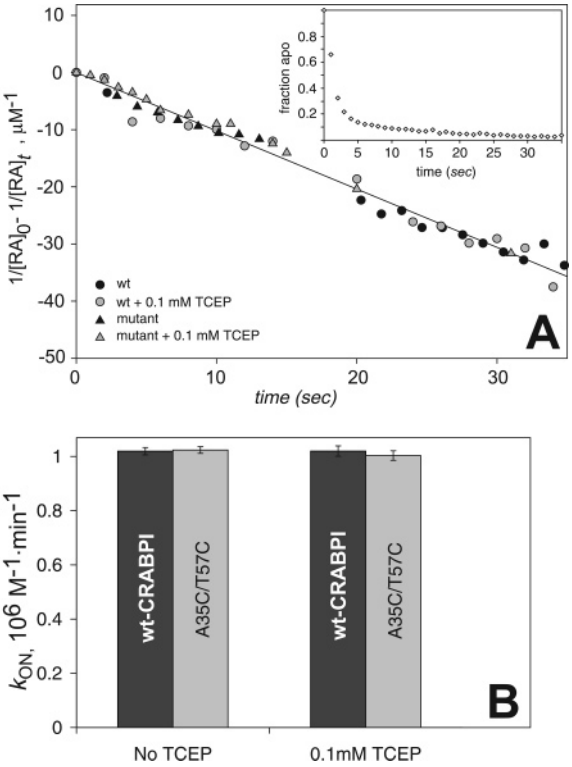

FIGURE 5: (A) RA association with wt-CRABP I and CRABP I A35C/T57C in the presence and absence of reducing agent. The negative of the slope of the plot is k_{on}, the rate constant of the association reaction (see the text for more details). (Inset) Raw fluorescence data for protein quenching due to binding of RA. (B) Values of k_{on} for wt-CRABP I (black bars) and CRABP I A35C/T57C (gray bars) in the absence and presence of reducing agent. Each value is the result of four different experiments.

form of the double mutant is 5.2 nM, which is in the range of previous reported values (*33*, *34*).

Increased Stability of the Mutant Protein−Ligand Complex in the Gas Phase. Previously we demonstrated that RA−CRABP I complex is only marginally stable in the gas phase and dissociates readily in the ESI interface, presumably due to the significant role played by the hydrophobic interactions in maintaining complex integrity (*35*). In this work, the effect of the double mutation on the stability of the protein−ligand complex was probed by monitoring the extent of dissociation as a function of the declustering potential in the ESI interface simultaneously for both wt-CRABP I and the double mutant. The results of these measurements (Figure 8) suggest that the double mutation results in a significant increase of the fraction of surviving protein−ligand complexes even at high declustering potential. Since RA dissociation in the gas phase is likely to involve (partial) unfolding of the host protein as a required step, the double mutation clearly enhances the protein conformational stability even in the absence of solvent.

DISCUSSION

The mechanisms of retinoic acid interaction with CRABPs have been the subject of extensive studies by X-ray crystallography (*19*), nuclear magnetic resonance (*12*), and mass spectrometry (*17*). These studies and those done on members of the iLBP family (*13*, *36*−*44*) have provided detailed information concerning the structure of the ligand-binding site, conformation of the β-barrel backbone side chains, and

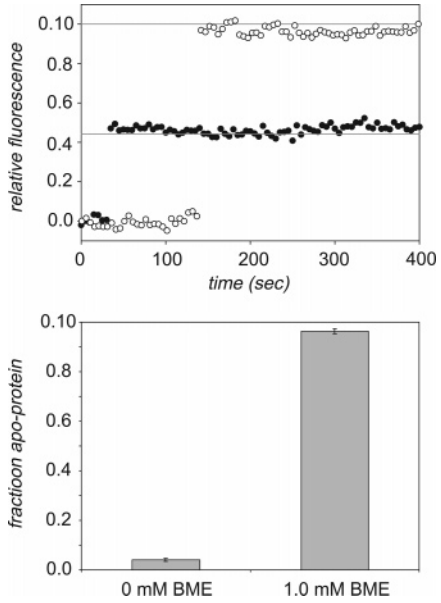

FIGURE 6: (Top) Fluorescence intensity change upon addition of holo-CRABP I A35C/T57C to the SUV with (●) and without (○) protein reduction prior to its mixing with SUV. The two horizontal lines on the graph represent the fluorescence level of the apo (lower) and holo (upper) forms of the protein, which were calculated with the assumption of no SUV−protein interaction. (Bottom) RA partitioning between CRABP I A35C/T57C and SUV in the presence and absence of the reducing agent. Values are the average of four independent measurements.

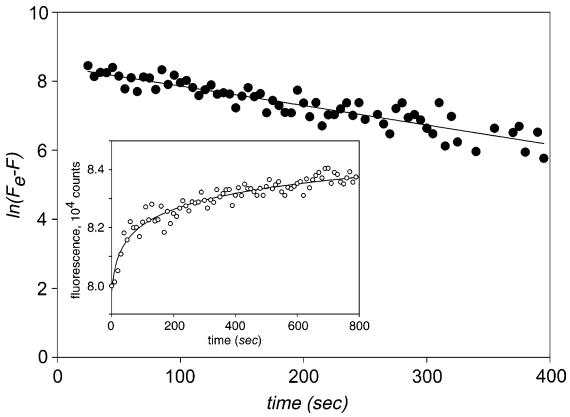

FIGURE 7: Representative plot for k_{off} measurement of RA from the reduced form of holo-CRABP I A35C/T57C. (Inset) Raw fluorometric data for transfer of RA from the reduced mutant protein to the DOPC vesicles.

dynamic motions of the protein essential for retinoic acid entrance into the cavity. These studies lead to a hypothesis that the region surrounding the βC−D loop, the βE−F loop, and the N-terminal region of helix II serve as an entry/exit port for the ligand (the so-called portal region hypothesis). This hypothesis gained further support from several studies aimed at modulating the kinetics of RA entry into the binding cavity by mutating residues in the portal region to increase the channel diameter (*14*, *45*, *46*). The objective of this study was different, as we sought to modulate the ligand-binding properties of CRABP I (more specifically, ligand exit from the cavity) by inhibiting the ligand exit from the cavity without affecting the entrance to the binding site. To achieve this objective, we engineered a CRABP I mutant in which the initial RA binding event triggers an irreversible covalent modification. This modification (cross-linking) arrests the

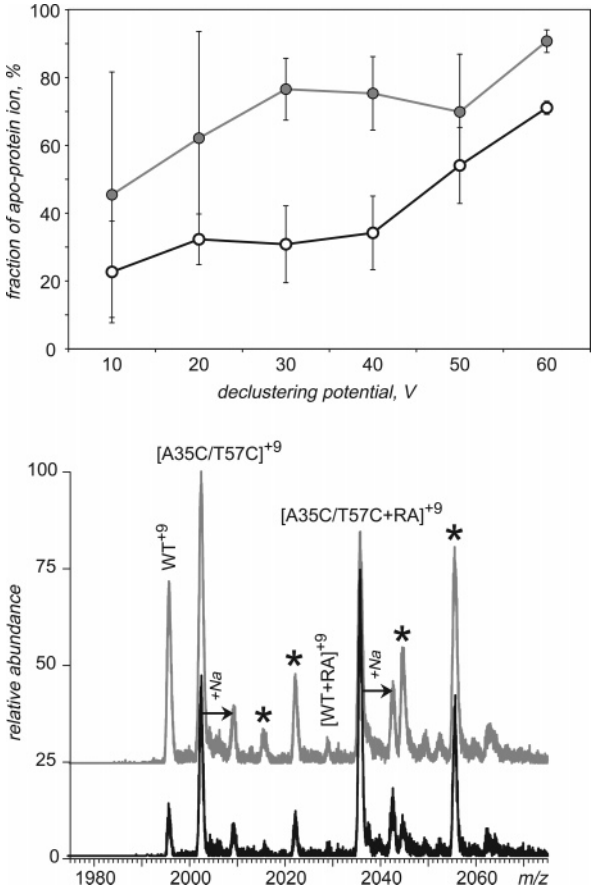

FIGURE 8: Stability of CRABP I complex with RA in the absence of solvent. (Top) Fraction of dissociated complexes as a function of declustering potential in the ESI interface for wild-type (gray circles) and double mutant CRABP I (open circles). (Bottom) Detailed view of the +9 region of the ESI mass spectra of holo forms of wild-type (gray trace) and double mutant (black trace) CRABP I, acquired at declustering potential 20 V.

large-scale dynamic motions of the protein backbone in the portal region, thereby preventing RA from exiting the binding cavity.

The residues mutated in this study were selected for several reasons. Crystal structure analysis of CRABP I in the apo and holo forms has shown that there are very few differences between the two conformations (*19*). The most significant one is the difference in the position of helix II with respect to the βC−D loop. The residues A35 (helix II) and T57 (βC−D loop) are not involved in ligand binding, although both appear to be highly conserved within the iLBP family. A35 is conserved in 19 proteins (36.5%) and T57 is conserved in 36 proteins (69.2%) among the 52 iLBP family members, and the nonconserved residues also have small side chains. [A35 is replaced by L (nine proteins), V (four proteins), T (10 proteins), I (seven proteins), and D (three proteins); T57 is replaced by P (four proteins), A (six proteins), G (three proteins), and N (one protein)]. Not surprisingly, substituting A35 and T57 in the CRABP I sequence with cysteine residues does not interfere with RA entry into the binding cavity, as the thiol side chains are too small to create any steric hindrance in the portal region and are pointing toward the outside of the protein. At the same time, a minor conformational adjustment in the portal region following RA binding to the protein brings the two residues in close enough proximity to afford disulfide bond formation

between the two newly introduced cysteine residues. Formation of the disulfide bond in the holo form and its absence in the apo form of the double mutant was confirmed by mass spectrometric methods.

While the mutations did not exert a significant influence on the protein stability in the absence of the ligand and its association rate, disulfide bond formation prevented RA from exiting the protein cavity in the absence of a reducing agent. When the latter was added to the holo-protein solution, the off rate was similar to that of the wild-type protein. Interestingly, the apo mutant form could refold back to its native conformation, whereas the denatured holo form of the protein could not be refolded back to its native conformation as shown by fluorescence spectroscopy. It is likely that the presence of a disulfide bond in the double mutant disturbs the protein energy landscape significantly enough to introduce a misfolded state acting as a kinetic trap. It remains to be seen whether the oxidized form of the refolded double mutant has a single conformation or is an ensemble of several conformations. This observation is very intriguing, since the previous studies of CRABP I folding showed that the helical segments were the first elements of higher-order structure to form (following less than 300 μs), to be followed later by the formation of the β-sheets (on the 100 ms scale) (*18*, *47*). It seems plausible that once the helices are formed, the disulfide bond locks the protein in an energetically favorable conformation that does not allow the β-sheets to form, trapping the protein in a misfolded state.

Despite its inability to properly fold from the denatured state, the ligand-bound oxidized form of the double mutant is remarkably stable and displays superior ligand-binding properties (compared to wt-CRABP I) even in the absence of solvent. While several mutants have been designed in the past on the basis of the iLBP template, modulation of the ligand binding affinity was achieved by adjusting the steric hindrance at the protein aperture leading to the internal cavity or by mutating residues that interact with RA in the ligand binding pocket. The double mutant presented and investigated in this work is unique in that the ligand locking in the binding cavity is achieved by arresting the dynamic fluctuations in the portal region.

The emergence of nanomedicine and molecular therapeutics in recent years has resulted in a surge of interest in designing macromolecules with precisely controlled properties. Although the majority of work in this field is now focused on nanocarriers as drug delivery vehicles (*48*), significant efforts are also invested toward designing constructs inspired by protein cage architectures, such as viral capsids (*49*, *50*). The approach presented in this work may be used to design highly specific and efficient sequestering agents for small molecules. The ligand trapping is irreversible due to formation of a covalent cross-link, which is triggered by the binding event itself. Since the release of the ligand and recycling of the "transporter-turned-trap" protein is only possible under reducing conditions, systems similar to the one presented in this work may also be used in biotechnological applications that require highly efficient monodirectional transport of small molecules (e.g., bioreactor-based manufacturing). Finally, the successful engineering of a CRABP I mutant that converts a transport protein to a trap provides conclusive evidence of validity of the portal hypothesis of ligand binding to proteins from the iLBP family.

ACKNOWLEDGMENT

We are grateful to Professor Lila M. Gierasch (University of Massachusetts-Amherst) for providing the wt-CRABP I plasmid.

SUPPORTING INFORMATION AVAILABLE

Sequence of CRABP I A35C/T57C and scoring of the disulfide bond by the disulfide by design program in the apo and holo forms of the mutant CRABP. This material is available free of charge via the Internet at http://pubs.acs.org.

REFERENCES

1. Chambon, P. (1996) A decade of molecular biology of retinoic acid receptors, *FASEB J. 10*, 940−954.
2. Ross, S. A., McCaffery, P. J., Drager, U. C., and De Luca, L. M. (2000) Retinoids in embryonal development, *Physiol. Rev. 80*, 1021−1054.
3. Ruhl, R., Plum, C., Elmazar, M. M., and Nau, H. (2001) Embryonic subcellular distribution of 13-*cis*- and *all-trans*-retinoic acid indicates differential cytosolic/nuclear localization, *Toxicol. Sci. 63*, 82−89.
4. Noy, N. (2000) Retinoid-binding proteins: mediators of retinoid action, *Biochem. J. 348* (Pt. 3), 481−495.
5. Roos, T. C., Jugert, F. K., Merk, H. F., and Bickers, D. R. (1998) Retinoid metabolism in the skin, *Pharmacol Rev 50*, 315−333.
6. Chomienne, C., Fenaux, P., and Degos, L. (1996) Retinoid differentiation therapy in promyelocytic leukemia, *FASEB J. 10*, 1025−1030.
7. Borghi, R., Vene, R., Arena, G., Schubert, D., Albini, A., and Tosetti, F. (2003) Transient modulation of cytoplasmic and nuclear retinoid receptors expression in differentiating human teratocarcinoma NT2 cells, *J. Neurochem. 84*, 94−104.
8. Mark, M., Ghyselinck, N. B., Wendling, O., Dupe, V., Mascrez, B., Kastner, P., and Chambon, P. (1999) A genetic dissection of the retinoid signalling pathway in the mouse, *Proc. Nutr. Soc. 58*, 609−613.
9. Sun, S. Y., Yue, P., Mao, L., Dawson, M. I., Shroot, B., Lamph, W. W., Heyman, R. A., Chandraratna, R. A., Shudo, K., Hong, W. K., and Lotan, R. (2000) Identification of receptor-selective retinoids that are potent inhibitors of the growth of human head and neck squamous cell carcinoma cells, *Clin. Cancer Res. 6*, 1563−1573.
10. Dong, D., Ruuska, S. E., Levinthal, D. J., and Noy, N. (1999) Distinct roles for cellular retinoic acid-binding proteins I and II in regulating signaling by retinoic acid, *J. Biol. Chem. 274*, 23695−23698.
11. Venepally, P., Reddy, L. G., and Sani, B. P. (1996) Analysis of the effects of CRABP I expression on the RA-induced transcription mediated by retinoid receptors, *Biochemistry 35*, 9974−9982.
12. Krishnan, V. V., Sukumar, M., Gierasch, L. M., and Cosman, M. (2000) Dynamics of cellular retinoic acid binding protein I on multiple time scales with implications for ligand binding, *Biochemistry 39*, 9119−9129.
13. Hodsdon, M. E., and Cistola, D. P. (1997) Discrete backbone disorder in the nuclear magnetic resonance structure of apo intestinal fatty acid-binding protein: implications for the mechanism of ligand entry, *Biochemistry 36*, 1450−1460.
14. Jenkins, A. E., Hockenberry, J. A., Nguyen, T., and Bernlohr, D. A. (2002) Testing of the portal hypothesis: analysis of a V32G, F57G, K58G mutant of the fatty acid binding protein of the murine adipocyte, *Biochemistry 41*, 2022−2027.
15. Hagan, R. M., Worner-Gibbs, J., and Wilton, D. C. (2005) Tryptophan insertion mutagenesis of liver fatty acid-binding protein: L28W mutant provides important insights into ligand binding and physiological function, *J. Biol. Chem. 280*, 1782−1789.
16. Falomir-Lockhart, L. J., Laborde, L., Kahn, P. C., Storch, J., and Corsico, B. (2006) Protein-membrane interaction and fatty acid transfer from intestinal fatty acid-binding protein to membranes. Support for a multistep process, *J. Biol. Chem. 281*, 13979−13989.
17. Xiao, H., and Kaltashov, I. A. (2005) Transient structural disorder as a facilitator of protein-ligand binding: native H/D exchange-

mass spectrometry study of cellular retinoic acid binding protein I, *J. Am. Soc. Mass Spectrom. 16*, 869−879.
18. Clark, P. L., Weston, B. F., and Gierasch, L. M. (1998) Probing the folding pathway of a beta-clam protein with single-tryptophan constructs, *Folding Des. 3*, 401−412.
19. Kleywegt, G. J., Bergfors, T., Senn, H., Le Motte, P., Gsell, B., Shudo, K., and Jones, T. A. (1994) Crystal structures of cellular retinoic acid binding proteins I and II in complex with *all-trans*-retinoic acid and a synthetic retinoid, *Structure 2*, 1241−1258.
20. Chrisman, P. A., and McLuckey, S. A. (2002) Dissociations of disulfide-linked gaseous polypeptide/protein anions: ion chemistry with implications for protein identification and characterization, *J. Proteome Res. 1*, 549−557.
21. Budhu, A. S., and Noy, N. (2002) Direct channeling of retinoic acid between cellular retinoic acid-binding protein II and retinoic acid receptor sensitizes mammary carcinoma cells to retinoic acid-induced growth arrest, *Mol. Cell. Biol. 22*, 2632−2641.
22. Hemsley, A., Arnheim, N., Toney, M. D., Cortopassi, G., and Galas, D. J. (1989) A simple method for site-directed mutagenesis using the polymerase chain reaction, *Nucleic Acids Res. 17*, 6545−6551.
23. Cogan, U., Kopelman, M., Mokady, S., and Shinitzky, M. (1976) Binding affinities of retinol and related compounds to retinol binding proteins, *Eur. J. Biochem. 65*, 71−78.
24. Clark, P. L., Liu, Z. P., Zhang, J., and Gierasch, L. M. (1996) Intrinsic tryptophans of CRABPI as probes of structure and folding, *Protein Sci. 5*, 1108−1117.
25. Fiorella, P. D., Giguere, V., and Napoli, J. L. (1993) Expression of cellular retinoic acid-binding protein (type II) in *Escherichia coli*. Characterization and comparison to cellular retinoic acid-binding protein (type I), *J. Biol. Chem. 268*, 21545−21552.
26. Noy, N., and Xu, Z. J. (1990) Interactions of retinol with binding proteins: implications for the mechanism of uptake by cells, *Biochemistry 29*, 3878−3883.
27. Zhang, J., Liu, Z. P., Jones, T. A., Gierasch, L. M., and Sambrook, J. F. (1992) Mutating the charged residues in the binding pocket of cellular retinoic acid-binding protein simultaneously reduces its binding affinity to retinoic acid and increases its thermostability, *Proteins: Struct., Funct., Genet. 13*, 87−99.
28. Creighton, T. E. (1990) Protein folding, *Biochem. J. 270*, 1−16.
29. Zhang, M., and Kaltashov, I. A. (2006) Mapping of protein disulfide bonds using negative ion fragmentation with a broadband precursor selection, *Anal. Chem. 78*, 4820−4829.
30. Noy, N., and Blaner, W. S. (1991) Interactions of retinol with binding proteins: studies with rat cellular retinol-binding protein and with rat retinol-binding protein, *Biochemistry 30*, 6380−6386.
31. Herr, F. M., Li, E., Weinberg, R. B., Cook, V. R., and Storch, J. (1999) Differential mechanisms of retinoid transfer from cellular retinol binding proteins types I and II to phospholipid membranes, *J. Biol. Chem. 274*, 9556−9563.
32. Sessler, R. J., and Noy, N. (2005) A ligand-activated nuclear localization signal in cellular retinoic acid binding protein-II, *Mol. Cell 18*, 343−353.
33. Fogh, K., Voorhees, J. J., and Astrom, A. (1993) Expression, purification, and binding properties of human cellular retinoic acid-binding protein type I and type II, *Arch. Biochem. Biophys. 300*, 751−755.
34. Sanquer, S., and Gilchrest, B. A. (1994) Characterization of human cellular retinoic acid-binding proteins-I and -II: ligand binding affinities and distribution in skin, *Arch. Biochem. Biophys. 311*, 86−94.
35. Xiao, H., Kaltashov, I. A., and Eyles, S. J. (2003) Indirect assessment of small hydrophobic ligand binding to a model protein using a combination of ESI MS and HDX/ESI MS, *J. Am. Soc. Mass Spectrom. 14*, 506−515.
36. Li, H., and Frieden, C. (2005) NMR studies of 4-^{19}F-phenylalanine-labeled intestinal fatty acid binding protein: evidence for conformational heterogeneity in the native state, *Biochemistry 44*, 2369−2377.
37. Rajabzadeh, M., Kao, J., and Frieden, C. (2003) Consequences of single-site mutations in the intestinal fatty acid binding protein, *Biochemistry 42*, 12192−12199.
38. Storch, J., Veerkamp, J. H., and Hsu, K. T. (2002) Similar mechanisms of fatty acid transfer from human anal rodent fatty acid-binding proteins to membranes: liver, intestine, heart muscle, and adipose tissue FABPs, *Mol. Cell. Biochem. 239*, 25−33.
39. Toke, O., Monsey, J. D., and Cistola, D. P. (2007) Kinetic mechanism of ligand binding in human ileal bile acid binding protein as determined by stopped-flow fluorescence analysis, *Biochemistry 46*, 5427−5436.
40. Tochtrop, G. P., DeKoster, G. T., Covey, D. F., and Cistola, D. P. (2004) A single hydroxyl group governs ligand site selectivity in human ileal bile acid binding protein, *J. Am. Chem. Soc. 126*, 11024−11029.
41. Lu, J., Cistola, D. P., and Li, E. (2003) Two homologous rat cellular retinol-binding proteins differ in local conformational flexibility, *J. Mol. Biol. 330*, 799−812.
42. Lu, J., Lin, C. L., Tang, C., Ponder, J. W., Kao, J. L., Cistola, D. P., and Li, E. (2000) Binding of retinol induces changes in rat cellular retinol-binding protein II conformation and backbone dynamics, *J. Mol. Biol. 300*, 619−632.
43. Lu, J., Lin, C. L., Tang, C., Ponder, J. W., Kao, J. L., Cistola, D. P., and Li, E. (1999) The structure and dynamics of rat apo-cellular retinol-binding protein II in solution: comparison with the X-ray structure, *J. Mol. Biol. 286*, 1179−1195.
44. Hodsdon, M. E., and Cistola, D. P. (1997) Ligand binding alters the backbone mobility of intestinal fatty acid-binding protein as monitored by ^{15}N NMR relaxation and ^{1}H exchange, *Biochemistry 36*, 2278−2290.
45. Zhang, F., Lucke, C., Baier, L. J., Sacchettini, J. C., and Hamilton, J. A. (2003) Solution structure of human intestinal fatty acid binding protein with a naturally-occurring single amino acid substitution (A54T) that is associated with altered lipid metabolism, *Biochemistry 42*, 7339−7347.
46. Richieri, G. V., Low, P. J., Ogata, R. T., and Kleinfeld, A. M. (1999) Binding kinetics of engineered mutants provide insight about the pathway for entering and exiting the intestinal fatty acid binding protein, *Biochemistry 38*, 5888−5895.
47. Clark, P. L., Liu, Z. P., Rizo, J., and Gierasch, L. M. (1997) Cavity formation before stable hydrogen bonding in the folding of a beta-clam protein, *Nat. Struct. Biol. 4*, 883−886.
48. Moghimi, S. M., Hunter, A. C., and Murray, J. C. (2005) Nanomedicine: current status and future prospects, *FASEB J. 19*, 311−330.
49. Georgens, C., Weyermann, J., and Zimmer, A. (2005) Recombinant virus like particles as drug delivery system, *Curr. Pharm. Biotechnol. 6*, 49−55.
50. Lee, L. A., and Wang, Q. (2006) Adaptations of nanoscale viruses and other protein cages for medical applications, *Nanomedicine 2*, 137−149.
51. Dombkowski, A. A. (2003) Disulfide by Design: a computational method for the rational design of disulfide bonds in proteins, *Bioinformatics 19*, 1852−1853.

BI700867C